

Iterative Learning Control for Precise Aircraft Trajectory Tracking in Continuous Climb and Descent Operations

Almudena Buelta, Alberto Olivares, and Ernesto Staffetti

Abstract—This paper presents an iterative learning control method for precise aircraft trajectory tracking. Given a trajectory to be followed by an aircraft with a dynamical model which is assumed to be known, the proposed algorithm improves the system performance in following the trajectory using the spatial and temporal deviations suffered by previous flights to anticipate recurring disturbances and compensate for them proactively by generating a new reference trajectory to be followed, which is the input for the aircraft’s own trajectory tracking controller. The proposed method is tested in a simulated busy terminal maneuvering area in which the time-based separation between aircraft is short enough for similar weather conditions to be expected. The numerical experiments are conducted considering aircraft of the same type, which are assumed to follow the same trajectory in two operations in which precise trajectory tracking is essential: continuous climb and descent operations. The obtained results show a significant reduction of the trajectory tracking error in few iterations, proving the effectiveness of the iterative learning control method applied to commercial aircraft trajectory tracking. Higher precision in trajectory tracking implies higher predictability of aircraft trajectories, which results in an improvement of the efficiency and capacity of the air traffic management system and in reductions of costs and emissions.

Index Terms—Aircraft Trajectory Tracking, Iterative Learning Control, Trajectory Predictability, Air Traffic Management, Trajectory Based Operations.

I. INTRODUCTION

THE global air navigation system is adapting to the expected increase in air traffic demand through international initiatives like the Single European Sky ATM Research¹ (SESAR) and the Next Generation Air Transportation System² (NextGen), the modernization efforts of which are enabling a new Air Traffic Management (ATM) paradigm built on four-dimensional (4D) trajectory-based operations (TBO), which allow for optimized trajectories, improving efficiency, predictability, and airspace capacity. 4D trajectories consist of the three spatial dimensions and the additional component of time, meaning that any delay is considered a deviation of the trajectory in the same way as a level change or a change of the horizontal position. Predictability is key to the implementation of TBO, requiring high precision in aircraft trajectory tracking to ensure safety and an efficient

exploitation of the airspace. Multiple random factors, such as unpredictable weather conditions (mainly wind and storms), hinder precision, resulting in deviations from the planned trajectory that can neither be predicted nor compensated by conventional aircraft trajectory tracking controllers, which, generally speaking, employ a feedback control scheme and react to disturbances as they occur [1, Chap. 1].

A. Previous approaches

The method here described addresses these limitations by using an Iterative Learning Control (ILC) scheme, which improves precision in trajectory tracking by incorporating error information from previous flights into the control law for subsequent aircraft performing the same planned trajectory, hence accurate performance can be achieved with a low transient tracking error despite recurrent disturbances. The widely recognized seminal work in ILC is [2], which generated a major area of research in control systems for robotics applications. Since then, ILC has broadened including links with other control paradigms. Non-linear ILC, robustness, adaptive schemes in ILC, the optimal control approach to ILC, and neural-network-based ILC are introduced in [3, Sect. 2] and references therein.

There is a vast array of literature associated with ILC, for instance the survey [4], where the main results in ILC analysis and design are discussed, and several textbooks such as [5], which treats ILC for both linear and nonlinear systems, and [6], which focuses on real time applications. Application areas have also expanded beyond industrial robotics and ILC has recently been applied to precise trajectory tracking of aerial robots. In [7], an ILC approach is applied to precise quadcopter trajectory tracking in the presence of model errors and other recurrent disturbances. In [8], a least-squares based learning rule is proposed to perform aggressive maneuvers with quadcopters. Other variants of ILC have been applied to trajectory tracking for Unmanned Aerial Vehicles (UAV), see for example [9] and references therein.

ILC shares some similarities with adaptive control. The key difference between them is that adaptive control strategies are on-line algorithms which modify the parameters of a system, the controller, whereas ILC are off-line algorithms which modify a signal, the commanded reference input for the process [4], [10]. The main adaptive control techniques include Model Reference Adaptive Control, Model Identification Adaptive Control, and Dual Adaptive Control [11]. Some

All authors are with Universidad Rey Juan Carlos, Fuenlabrada, Spain (e-mail: almudenajose.buelta@urjc.es; alberto.olivares@urjc.es; ernesto.staffetti@urjc.es).

¹<https://www.sesarju.eu/>

²<https://www.faa.gov/nextgen/>

recent publications in which adaptive control strategies are applied to aircraft trajectory tracking are [12], [13], and [14]. In [15], adaptive control has been used in combination with ILC to improve performance in tracking the trajectory of a quadcopter.

The application of ILC to precise aircraft trajectory tracking requires information about the intended and actually flown trajectories of previous aircraft in the relevant airspace. This information is assumed here to be available, and it will actually become accessible with the implementation of System Wide Information Management (SWIM). This project is part of the ICAO Global Air Navigation Plan [16, Appx. 2] and consists of the standards, infrastructure, and governance enabling information exchange among the different ATM stakeholders, including aeronautical, weather, and flight data.

This paper can be considered an extension of [17] and [18], where the optimization-based ILC method presented in [7] is proven to improve precision in aircraft trajectory tracking in Continuous Climb Operations (CCO) and Continuous Descent Approaches (CDA), respectively, by pure feed-forward adaptation of the control input. This ILC scheme combines optimal filtering for disturbance estimation with optimization techniques that determine an updated control input, resulting in an effective and computationally efficient learning strategy. This method relies on a nominal model of the aircraft in which input and state constraints are explicitly taken into account. In this paper, several improvements have been introduced with respect to [17] and [18]. The simulated environment in which the experiments have been conducted is more accurate than in [17] and [18]. A more realistic wind model has been used, in which wind turbulence has been considered, a constrained Kalman filter for smooth disturbance estimation has been employed, which is able to reject the turbulence effect, and an aircraft model has been considered, in which some of the state variables are assumed to be not directly measurable. However, the most important improvement with respect to [17] and [18] is the use of an ILC strategy that generates a new reference trajectory for the aircraft's underlying trajectory tracking feedback controller, instead of directly acting on the aircraft's control inputs. An optimization-based Indirect Iterative Learning Control (IILC) has been employed for this purpose. An overview of IILC can be found in [19]. It is a variant of the ILC strategy that, unlike ILC, which directly alters the open-loop input to the system, modifies the reference trajectory given to a feedback controller, which then converts this trajectory into system control inputs. One advantage of using the IILC method is that it is nonintrusive with respect to the underlying trajectory tracking control system of the aircraft, since a new reference trajectory can be computed as part of the input update and fed into the flight management system of the following aircraft. In this way, the feedback trajectory tracking control reduces nonrepetitive disturbances while the IILC is intended to reject repetitive disturbances. This IILC scheme requires the system dynamics to be repetition-invariant, therefore it is assumed that the same aircraft aims to perform the same planned trajectory at each iteration. In a more realistic scenario, consecutive flights along the same path are generally carried out by different aircraft and follow

different trajectories. The knowledge transfer problem among dynamical systems and among trajectories is not addressed in this paper and will be the subject of future research.

The experiments of which the results are reported in this paper were carried out in a simulated environment. A realistic scenario has been built in MATLAB/Simulink, a graphical programming environment for modeling and simulating dynamical systems developed by MathWorks³. This scenario includes a flight simulator composed of an aircraft model, for which commercial aircraft data from the Base of Aircraft Data (BADA) has been used, and an aircraft proportional-integral feedback controller, which emulates the aircraft trajectory tracking controller. BADA is an Aircraft Performance Model (APM) developed and maintained by EUROCONTROL⁴ with the collaboration of aircraft manufacturers and airlines, specifically designed for the simulation and prediction of aircraft trajectories for research and operations in ATM. The BADA APM has two components: model specifications, which provide the theoretical models used to calculate aircraft performance parameters, and data sets, which give the aircraft-specific coefficients. There are two families of the BADA APM, based on the same modeling approach and with the same components: BADA Family 3 and BADA Family 4. The latest release of the former has been used in this paper [20, Chaps. 3, 5].

Improving precision in trajectory tracking is crucial in busy air spaces like Terminal Maneuvering Areas (TMA), where high traffic density requires accurate predictability of aircraft trajectories in order to avoid conflicts between arriving and departing flows. IILC is especially suitable in TMA, since the time between flights with similar planned routes is short enough to expect negligible variations in weather conditions and therefore assume similar disturbances. In particular, the IILC paradigm has been studied for CCO and Continuous Descent Operations (CDO)⁵, in which it is assumed that the execution of a vertical flight profile optimized to the performance of the aircraft is allowed, leading to significant reduction of fuel consumption and environmental benefits in terms of noise and emissions. In general, CCO are part of a Standard Instrument Departure (SID) procedure [22, Chap. 1], and CDO are part of a Standard Terminal Arrival Route (STAR) procedure, in which case they are known as Optimized Profile Descents (OPD) [23, Chap. 1]. In this paper, feasible CCO and CDO aircraft trajectories have been generated using a pseudospectral optimal control approach [24].

B. Contributions of the paper

In this paper, an optimization-based ILC scheme has been applied to precise trajectory tracking for commercial fixed-wing aircraft flying in realistic operational scenarios, proving the effectiveness of this approach to compensate for disturbances on these systems in the presence of operational constraints despite being much larger, less maneuverable, and having

³<https://es.mathworks.com/>

⁴<https://www-test.eurocontrol.int/services/bada>

⁵According to [21], the terms CDO and CDA are interchangeable and should be read and understood in the same context.

a slower control response than rotary-wing small UAV, the only aerial systems in which the ILC method had already been tested. To the best knowledge of the authors, ILC has only been applied to commercial aircraft trajectory tracking in their previous works [17] and [18], to which this article is an extension. The advantage of the optimization-based ILC method used in the experiments is that the disturbance estimation and the input update steps are clearly separated, allowing for intuitive tuning of the overall learning scheme and a flexible combination of different approaches for both steps [7]. The constrained Kalman filter explicitly takes noise characteristics into account, and can be adjusted to improve the convergence and smoothness of the estimation. The input update is formulated as a convex optimization problem in which input and state constraints can be explicitly incorporated. The objective function can include derivatives of the input to reduce jittering in the control inputs and, consequently, improve the robustness of the learning.

Additionally, a specific ILC scheme, the IILC, has been designed, which is suitable for being implemented on commercial aircraft since it allows for repetitive disturbance corrections without interfering with the aircraft's existing trajectory tracking controller, simply by generating, at each iteration, a new reference trajectory to be followed by the aircraft instead of a new control input. This means that the IILC controller can be physically implemented on a supplementary system which can be equipped without changing the avionics of the aircraft. This represents a great advantage for airlines interested in retrofitting this technology.

The application of the IILC technique to precise aircraft trajectory tracking is an innovative solution to increase the predictability of trajectories in the future TBO paradigm. Higher trajectory predictability implies an improvement of the efficiency and capacity of the ATM system. Airlines can also benefit from higher trajectory predictability by reducing the number of alterations in following the planned aircraft trajectories, which is associated with a reduction of costs and emissions.

C. Organization of the paper

The paper is organized as follows: the model of the aircraft dynamics is derived in Section II, including the feedback controller design and the wind model used in the simulations. The general IILC scheme is presented in Section III. The experiments carried out to test the IILC algorithm are described in Section IV, where the corresponding numerical results are reported and analyzed. Finally, Section V contains the conclusions.

II. AIRCRAFT DYNAMICS

This section describes the dynamic model of the aircraft used in the simulated environment.

A. Equations of motion

A common three-degrees-of-freedom dynamic model has been used, which describes the point variable-mass motion of the

aircraft over a non-rotating flat Earth model [25, Chap. 2]. In particular, a symmetric flight has been considered. Thus, it has been assumed that there is no sideslip and all forces lie in the plane of symmetry of the aircraft. In this work, IILC is used for precise trajectory tracking of the vertical profile of a CCO and a CDO. Therefore, the motion of the aircraft is limited to a vertical plane, i.e., with a constant course and thus a constant heading angle. Without loss of generality, it is assumed that the heading angle is zero. We also suppose that the aircraft performs a leveled wing flight, thus the bank angle is zero. The following equations of motion of the aircraft have been considered:

$$\begin{aligned}\dot{V}(t) &= \frac{T(t) - D(h_e(t), V(t), C_L(t)) - m(t) \cdot g \cdot \sin \gamma(t)}{m(t)}, \\ \dot{\gamma}(t) &= \frac{L(h_e(t), V(t), C_L(t)) - m(t) \cdot g \cdot \cos \gamma(t)}{m(t) \cdot V(t)}, \\ \dot{x}_e(t) &= V(t) \cdot \cos \gamma(t), \\ \dot{h}_e(t) &= V(t) \cdot \sin \gamma(t), \\ \dot{m}_{climb}(t) &= -T(t) \cdot \eta(V(t)), \quad \text{or} \quad \dot{m}_{descent}(t) = -f_{min}(h_e(t)).\end{aligned}\tag{1}$$

The dynamic equations in (1) are expressed in an aircraft-attached reference frame and the kinematic equations are expressed in a ground-based reference frame.

The state variables of the system (1) are the true airspeed, V , the flight path angle, γ , the horizontal position, x_e , the altitude, h_e , and the aircraft mass, m . Thus, the state vector is $\mathbf{x}(t) = (V(t), \gamma(t), x_e(t), h_e(t), m(t))$. The control inputs are the engine thrust, T , and the lift coefficient, C_L . Thus, the control vector is $\mathbf{u}(t) = (T(t), C_L(t))$. Lift, $L = C_L S \hat{q}$, and drag, $D = C_D S \hat{q}$, are the components of the aerodynamic force. Parameter S is the reference wing surface area and $\hat{q} = \frac{1}{2} \rho V^2$ is the dynamic pressure. A parabolic drag polar $C_D = C_{D0} + K C_L^2$ and an International Standard Atmosphere (ISA) model are assumed. The lift coefficient, C_L , is a known function of the angle of attack and the Mach number. Parameter η is the fuel efficiency coefficient and f_{min} is the minimum fuel flow corresponding to idle thrust descent conditions.

The state variables may not be directly measurable. In this model, the output variables are

$$\mathbf{y}(t) = (V_{IAS}(t), M(t), x_e(t), h_e(t), \dot{h}_e(t)),$$

where V_{IAS} is the indicated speed, M is the Mach number, x_e is the horizontal position, h_e is the altitude, and \dot{h}_e is the altitude rate. V_{IAS} and M are defined as:

$$\begin{aligned}V_{IAS}(t) &= a_0 \sqrt{\frac{2}{\kappa - 1} \left(\left(\frac{p(h_e(t))}{p_0} \left[\left(1 + \frac{\kappa - 1}{2} M(t)^2 \right)^{\frac{\kappa}{\kappa - 1}} - 1 \right] + 1 \right)^{\frac{\kappa - 1}{\kappa}} - 1 \right)}, \\ M(t) &= \frac{V(t)}{a(h_e(t))}.\end{aligned}\tag{2}$$

In (2), a , a_0 , p , and p_0 are the local and sea-level speed of sound and pressure, respectively, and κ is the adiabatic index of air.

B. Flight envelope constraints

Flight envelope constraints are derived from the geometry of the aircraft, structural limitations, engine power, and aerodynamic characteristics. The performance limitations model and the parameters have been obtained from BADA.

$$\begin{aligned}
 0 \leq h_e(t) &\leq \min[h_{M_0}, h_u(t)], & \gamma_{min} &\leq \gamma(t) \leq \gamma_{max}, \\
 M(t) &\leq M_{M_0}, & m_{min} &\leq m(t) \leq m_{max}, \\
 \dot{V}(t) &\leq a_l, & C_v V_s(t) &\leq V(t) \leq V_{M_0}, \\
 \dot{\gamma}(t)V(t) &\leq a_n, & 0 &\leq C_L(t) \leq C_{L_{max}}, \\
 T_{min}(t) &\leq T(t) \leq T_{max}(t).
 \end{aligned} \quad (3)$$

In (3), h_{M_0} is the maximum operational altitude and $h_u(t)$ is the maximum operative altitude at a given mass (it increases as fuel is burned). $M(t)$ is the Mach number and M_{M_0} is the maximum operating Mach number. C_v is the minimum speed coefficient, $V_s(t)$ is the stall speed, V_{M_0} is the maximum operating Calibrated Airspeed (CAS), and a_n and a_l are the maximum normal and longitudinal accelerations for civilian aircraft, respectively. Finally, $T_{min}(t)$ and $T_{max}(t)$ correspond to the minimum and maximum available thrust, respectively. To perform an optimized descent, the throttle should be near the idle detent position. Then, the minimum and maximum thrust constraints in descent in (3) are the thrust idle plus a negative and a positive margin, respectively.

C. Simulated feedback controller

As explained in the Introduction, one of the advantages of using IILC is that it does not interfere with the aircraft's existing feedback controller for trajectory tracking in the sense that, at each iteration, a new trajectory to be followed by the aircraft is generated instead of a new control input. Therefore, to test the effectiveness of the IILC method with a more realistic aircraft model, a proportional-integral (PI) feedback controller for trajectory tracking has been designed and included as part of the simulated aircraft used to conduct the experiments.

PI and PID control are very common feedback control methods (see for example [26] and [27]). Here, a PI feedback controller has been employed to stabilize the aircraft and drive it along a prescribed trajectory. When dealing with the aircraft's longitudinal dynamics, proportional control using the appropriate output error is usually sufficient to achieve the desired dynamic response. Integral control is then added to eliminate steady-state error (see [28, Chap. 4]).

The longitudinal dynamics characterize the forward speed and altitude of the aircraft. Driving them to some set values simultaneously requires feedback control of both the thrust and the lift coefficient. To select the most suitable output variables to provide feedback while keeping the system stable, the effect on the modal properties of the system of feeding back each control variable with each output has been analyzed. As a result of this analysis, the chosen strategy is to provide Mach feedback to the throttle and altitude rate feedback to the lift coefficient. To avoid excessive control effort, the speed rate is limited and, instead of direct altitude feedback, the altitude

error is used to determine an appropriate value for the altitude rate.

D. Wind model

Environmental disturbances have been simulated to test the IILC efficiency under realistic conditions such as those that may be experienced by the aircraft during flight. The current model provides the combined effect of mean horizontal wind speed and Dryden turbulence using built-in MATLAB functions⁶. The wind in the vertical direction has been assumed to be zero.

The mean horizontal wind model has been simulated using the U.S. Naval Research Laboratory Horizontal Wind Model routine [29], which describes the atmosphere's vector wind fields from the surface to the exobase as a function of latitude, longitude, altitude, day of year, and time of day. The empirical formulation, based on the utilization of both satellite and ground-based data sets, properly resolves the thermospheric wind patterns and is able to represent the predominant variations of the middle and upper atmosphere to an acceptable degree of accuracy. In this model, significant changes in the mean horizontal wind speed are only observable over long time periods, making the hypothesis of similar weather conditions between aircraft operations realistic.

The Dryden wind turbulence model uses an empirical spectral representation to add speed fluctuations to the mean speed, treating the linear and angular velocity components of continuous gusts as spatially varying stochastic processes. The inputs to the Dryden model are altitude, aircraft velocity, and direction cosine matrix. In this article, the mathematical representation implemented in the Military Specification MIL-F-8785C [30] has been used.

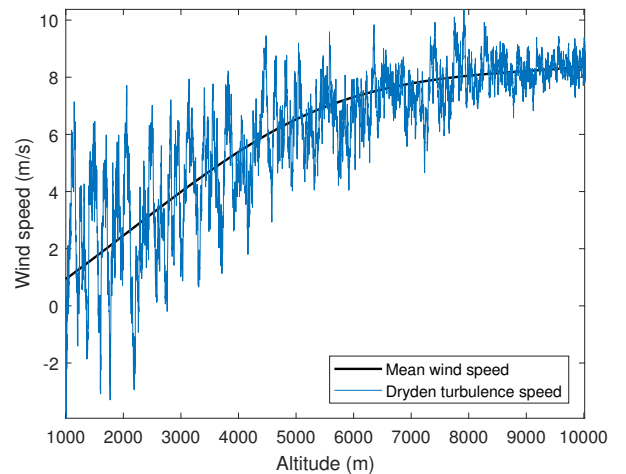


Fig. 1: Horizontal wind speed model.

The wind model used in the experiments combines repetitive and nonrepetitive disturbances, allowing the effectiveness of the described method to be proven through the combined efforts of the IILC, which compensates for the repetitive

⁶<https://es.mathworks.com/help/aeroblks/wind.html>

disturbances like the mean horizontal wind speed, and the feedback controller, which compensates for the nonrepetitive disturbances, like the wind turbulence. Figure 1 shows a realization of the wind speed when performing the CCO described in Section IV-A.

III. ITERATIVE LEARNING

In this section, following [7], the ILC method implemented in this paper for precise aircraft trajectory tracking will be introduced. The starting point of the learning algorithm is a time-varying nonlinear model of the real dynamic system

$$\begin{aligned}\dot{x}(t) &= f(x(t), u(t), t), \\ y(t) &= g(x(t), u(t), t),\end{aligned}\quad (4)$$

where $u(t) \in \mathbb{R}^{n_u}$ is the control input, $x(t) \in \mathbb{R}^{n_x}$ is the state, $y(t) \in \mathbb{R}^{n_y}$ is the output, and f and g are assumed to be continuously differentiable in x and u . Constraints on the input, $u(t)$, and the state, $x(t)$, as well as their time derivatives are represented by

$$Z q(t) \leq q_{max}, \quad (5)$$

where

$$q(t) = \left[x(t), u(t), \dot{x}(t), \dot{u}(t), \dots, \frac{d^m}{dt^m} x(t), \frac{d^m}{dt^m} u(t) \right] \quad (6)$$

and $q_{max} \in \mathbb{R}^{n_q}$. The inequality denoted by the symbol \leq is defined component-wise, n_q is the total number of constraints and Z is a constant matrix of appropriate dimensions. In this case, the time-varying nonlinear model of the aircraft and its constraints are described in Section II.

The goal of the presented learning algorithm is to track a feasible predefined output trajectory $y_d(t)$ precisely over a finite time interval $t \in \mathcal{T} = [t_0, t_f]$, with $t_f < \infty$. The desired output trajectory $y_d(t)$ and its corresponding state, $x_d(t)$, and control, $u_d(t)$, are here the result of solving an optimal control problem based on the system dynamics (1). As described in Section IV, the optimal control problems for generating the CCO and CDO desired trajectories have been solved using a pseudospectral method.

One useful way of describing the model dynamics during a single iteration is the lifted system representation, which consists of mapping the finite input time series into the corresponding output time series for each trial [31] after linearizing the system's behavior (4) about the desired trajectory and discretizing the resulting equations. Using this notation, the system (4) can be described as

$$\begin{aligned}x_j &= F u_j + d_j, \\ y_j &= G x_j + H u_j,\end{aligned}\quad (7)$$

where the subscript j indicates the j th execution of the desired task. For each iteration j , the triple (x, u, y) represents the lifted vectors describing small deviations from the desired trajectory and its corresponding state and input $(x_d(t), u_d(t), y_d(t))$, that is,

$$\begin{aligned}u &= [\tilde{u}(0), \tilde{u}(1), \dots, \tilde{u}(N-1)]^T \in \mathbb{R}^{N n_u}, \\ x &= [\tilde{x}(1), \tilde{x}(2), \dots, \tilde{x}(N)]^T \in \mathbb{R}^{N n_x}, \\ y &= [\tilde{y}(1), \tilde{y}(2), \dots, \tilde{y}(N)]^T \in \mathbb{R}^{N n_y},\end{aligned}\quad (8)$$

with $\tilde{u}(k) = u(k) - u_d(k)$,
 $\tilde{x}(k) = x(k) - x_d(k)$,
 $\tilde{y}(k) = y(k) - y_d(k)$,

where $k \in \mathcal{K} = \{0, 1, \dots, N\}$, with $N < \infty$, represents the discrete-time index.

The lifted matrices $F \in \mathbb{R}^{N n_x \times N n_u}$, $G \in \mathbb{R}^{N n_y \times N n_x}$, and $H \in \mathbb{R}^{N n_y \times N n_u}$ represent the model nominal dynamics. Vector d_j captures the repetitive disturbances along the reference trajectory, including model errors and the free response of the system to the initial deviation. d_j experiences only slight random changes, ω_j , between iterations. Taking into account process and measurement noise, captured in the random variable μ_j , the evolution of the learning over consecutive trials can be represented as a Kalman filter model [32, Chap. 5.2]

$$\begin{aligned}d_j &= d_{j-1} + \omega_{j-1}, \\ y_j &= G d_j + (G F + H) u_j + \mu_j,\end{aligned}\quad (9)$$

where both stochastic zero-mean Gaussian white noise variables, $\omega_j \sim \mathcal{N}(0, \Omega_j)$ and $\mu_j \sim \mathcal{N}(0, M_j)$, are trial-uncorrelated and assumed to be independent. Matrices Ω_j and M_j represent the noise covariances and can be characterized as diagonal matrices. In the aircraft simulation used for this study, noise has been introduced as measurement errors and variations in both the aircraft model and the wind speed.

The Kalman filter estimates the current error, d_j , taking into account the output signals y_0, y_1, \dots, y_j from previous trials. Given the initial values of the error estimate, \hat{d}_0 , and the error covariance matrix, $P_0 = E[(d_0 - \hat{d}_0)(d_0 - \hat{d}_0)^T]$, the disturbance estimate is calculated as

$$\hat{d}_j = \hat{d}_{j-1} + K_j (y_j - G \hat{d}_{j-1} - (G F + H) u_j), \quad (10)$$

where K_j is the optimal Kalman gain

$$K_j = (P_{j-1} + \Omega_{j-1}) G^T (G (P_{j-1} + \Omega_{j-1}) G^T + M_j)^{-1}. \quad (11)$$

Knowledge of the disturbance behavior can be incorporated into the Kalman filter in the form of equality and inequality constraints to improve its performance [33]. In this case, disturbance variation over time is bounded to obtain a smooth estimation of the mean horizontal wind speed while dismissing the turbulence effect, which varies over iterations.

Constraints can be addressed projecting the unconstrained estimate of the Kalman filter onto the constraint surface. The constrained disturbance estimation can therefore be written as a quadratic programming problem

⁷Note that the notation $\mathbb{R}^{N n_u}$ refers to the real vector space which dimension is the scalar product $N \cdot n_u$. It is defined analogously in all the vectors where this notation appears throughout this article.

$$\begin{aligned} \min_{\widehat{d}_{j,c}} \quad & (\widehat{d}_{j,c} - \widehat{d}_j)^T W (\widehat{d}_{j,c} - \widehat{d}_j) \\ \text{subject to} \quad & C \widehat{d}_{j,c} \leq c_{max}, \end{aligned} \quad (12)$$

where C is a matrix of appropriate dimension and c_{max} is the maximum allowed variation of the disturbance. W is a positive-definite weighting matrix. Setting $W = P_j$ provides the maximum probability estimates if the process and measurement noises are Gaussian.

The learning update consists in deriving a model-based update rule that computes a new control input $u_{j+1} \in \mathbb{R}^{N_{u}}$ in response to the estimated disturbance \widehat{d}_j , that is, minimizing the deviation from the nominal trajectory in the next trial. It can be expressed by the optimization problem

$$\begin{aligned} \min_{u_{j+1}} \quad & \|F u_{j+1} + \widehat{d}_{j,c}\|_{\ell} + \alpha \|D u_{j+1}\|_{\ell} \\ \text{subject to} \quad & L u_{j+1} \leq q_{max}, \end{aligned} \quad (13)$$

where constraints (5) are explicitly taken into account and $\alpha \geq 0$ and the matrix D are intended to penalize the input or approximations of its derivatives in order to enforce the smoothness of the optimal problem solution. In the experiments included in this article, the vector norm $\ell = 2$ has been chosen.

The update law defined in (13) can be formulated as a standard convex optimization problem, solved in this paper using CPLEX for MATLAB⁸, which provides a tool for solving optimization or mathematical programming problems, including quadratic and quadratically constrained problems.

A scaling of the original signals $u(t), x(t), y(t)$ in (4) is essential to guarantee reasonable results in the optimization problem. The scaling, exemplarily shown on the system's state $x(t)$, reads as

$$x^s = S_x x, \quad S \in \mathbb{R}^{N_{n_x} \times N_{n_x}}, \quad (14)$$

with x^s representing the scaled version of a lifted state vector x and S being the corresponding scaling matrix, usually represented by a diagonal matrix. Additionally, a state weighting matrix may be useful to give greater importance to some of the state variables over the rest. In the experiments shown in this paper, the position state variables (h_e and x_e) have been given greater importance than the rest. Additionally, the scaling along the trajectory has been modified in order to weight some parts of the trajectory more than others.

As mentioned in the introduction, one of the advantages of the indirect variant of the iterative learning algorithm is its nonintrusiveness with respect to the aircraft's existing trajectory tracking controller, since a new reference trajectory is provided to the following aircraft rather than a control input. Once the updated input, u_{j+1} , is calculated in (13), the new reference trajectory is obtained by introducing this input into the lifted model, dismissing the disturbances except for the initial deviation error

$$\begin{aligned} x_r &= F u_{j+1} + d_{j+1}^0 + x_d, \\ y_r &= G x_r + H u_{j+1} + y_d, \end{aligned} \quad (15)$$

where $x_r \in \mathbb{R}^{N_{n_x}}$ and $y_r \in \mathbb{R}^{N_{n_y}}$ are the new reference state and output lifted vectors, and $x_d \in \mathbb{R}^{N_{n_x}}$ and $y_d \in \mathbb{R}^{N_{n_y}}$ are the desired state and output vectors also in a lifted form. The reference trajectory to be fed into the system's feedback controller can be obtained from the unlifted representation form of x_r and y_r .

IV. NUMERICAL RESULTS

To show the effectiveness of the ILC method applied to precise aircraft trajectory tracking, the following two simulated experiments have been carried out:

- Experiment 1: Precise trajectory tracking in a Continuous Climb Operation.
- Experiment 2: Precise trajectory tracking in a Continuous Descent Operation.

A feasible trajectory with its corresponding nominal input is the starting point of the iterative learning algorithm. In both experiments, the feasible trajectories to be followed by the simulated aircraft have been generated using a pseudospectral optimal control method. Thus, not only feasible but also optimal aircraft trajectories have been obtained together with the optimal control inputs to steer the aircraft along them. Besides the optimal solution, the Hamiltonian, costates, path covectors, and endpoint covectors have been also computed for validation and verification of the solutions. In both experiments, the aircraft model and flight envelope used to generate the trajectories are those described in Section II, assuming zero wind.

As summarized in Figure 2, the simulated environment in which the experiments have been carried out is composed of two main blocks:

- a realistic flight simulator, which includes the aircraft model and a feedback controller, and
- an ILC controller, composed of an estimator of the disturbances acting on the aircraft and a nonlinear programming solver that provides the updated reference trajectory for the next iteration.

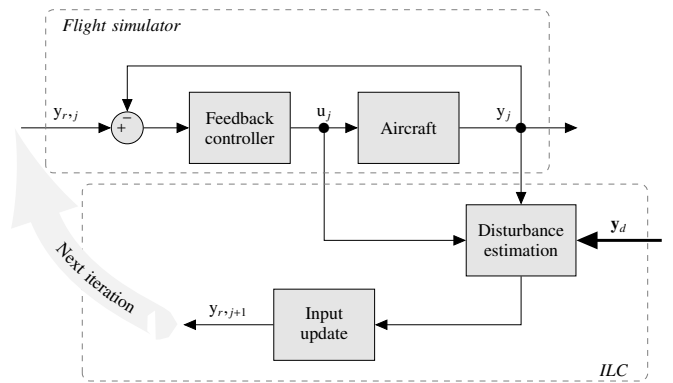


Fig. 2: Simulated environment scheme.

The flight simulator has been developed using a 3-DOF longitudinal model of an Airbus A320 aircraft implemented in Simulink, a software widely used in aircraft simulation [34]. The state, output, and control variables are those described in previous sections. This aircraft model has been designed

⁸<https://www.ibm.com/support/knowledgecenter/SSSA5P>

to include perturbations such as a realistic wind profile, model uncertainties, and measurement errors, and does not coincide with the nominal model used to calculate the optimal desired trajectories, in which perturbations are not taken into account. Additionally, to test the robustness of the algorithm to modeling errors, the aircraft parameters entered in the ILC controller are also slightly different from those used in the flight simulator and in the trajectory planning.

The IILC algorithm, which has been implemented in MATLAB, is summarized in Algorithm 1. The desired trajectory, y_d , state, x_d , and the corresponding input, u_d , are loaded from a file generated in the trajectory planning phase in Step 1. In the simulation stage, and using the latest feed-forward input generated by the IILC algorithm, the corresponding reference trajectory is fed into the aircraft controller and the resulting output is generated by the flight simulator. In the ILC stage, the resulting error vector is provided to a Kalman filter that estimates the tracking error, as described in Section III. Finally, based on the estimated tracking error, the update Step 10 of the learning algorithm is executed, which determines a new reference trajectory to be tracked in the next iteration, optimally compensating for the estimated error.

Algorithm 1 Summary of the IILC algorithm

INITIALIZATION

- 1: Load the trajectory to be followed and its corresponding nominal state and input $(x_d(t), u_d(t), y_d(t))$.
- 2: Linearize the system about the desired trajectory and convert it to a discrete-time system.
- 3: Note the system as a lifted domain representation (7), (8).
- 4: Enter the Kalman filter initial parameters and compute the Kalman gains (11).

AT EACH ITERATION

• Simulation stage

- 5: Set the simulated aircraft to the initial position.
- 6: Enter the reference trajectory into the feedback controller.
- 7: Simulate the flight with disturbances.

• ILC stage

- 8: Compare the output of the flight simulator with the desired trajectory.
 - 9: Estimate the tracking error (10), (12).
 - 10: Update the reference trajectory (13).
-

A. Experiment 1: Precise trajectory tracking in a Continuous Climb Operation

In this experiment, the trajectory to be followed by the simulated aircraft is a CCO.

1) Planning the CCO trajectory to be tracked

In [22, Chap. 1], ICAO defines CCO as “an aircraft operating technique enabled by airspace design, procedure design, and facilitation by ATC, allowing the execution of a flight profile optimized to the performance of the aircraft.” They also enumerate some advantages of CCO, such as more fuel efficient operations, reduction in both flight crew and controller workload through the design of procedures requiring less

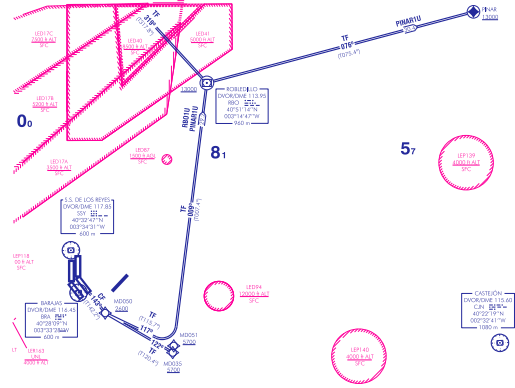


Fig. 3: SID PINAR1U. Source: Spanish AIP service. Not for operational use.

ATC intervention, reduction in the number of required radio transmissions, cost savings and environmental benefits through reduced fuel burn, potentially aircraft noise mitigation through thrust and height optimization, and potential authorization of operations where noise limitations would otherwise result in operations being curtailed or restricted. In this type of operations, precise trajectory tracking is essential to avoid potential conflict between traffic flows and ensure that safety and capacity are not compromised.

A CCO trajectory in the vertical plane associated with a SID procedure has been generated solving an optimal control problem in which fuel consumption has been minimized. Therefore, airspace constraints that represent the passage through the waypoints that define the SID are introduced in the trajectory generation problem together with the flight envelope constraints. The ILC algorithm has been tuned to give greater importance to the part of the trajectory comprising the waypoints than the rest of it by giving more weight to these points in the scaling matrix described in Section III. The boundary conditions for the state variables have been selected according to a realistic flight from the Adolfo Suárez Madrid-Barajas (LEMD) airport. The trajectory generation starts up at 1000 m after takeoff and ends at 10000 m, when the aircraft reaches the cruise level. Initial velocity and path angle have been selected according to standard values.

TABLE I: Coordinates of waypoints and nav aids of the SID PINAR1U. Source: Spanish AIP service.

Point	Type	Latitude	Longitude
MD050	RNAV waypoint	40°25'54.0220" N	003°29'37.3611" W
MD051	RNAV waypoint	40°22'15.4740" N	003°19'44.9769" W
RBO	DVOR/DME nav aid	40°51'14" N	003°14'47" W
PINAR	RNAV waypoint	40°58'49.0620" N	002°35'56.9980" W

The selected SID procedure is Madrid Barajas PINAR1U shown in Figure 3. The definition of the SID can be found in the Spanish Aeronautical Information Publication (AIP) service⁹, managed by ENAIRE, where the SID is textually described as follows: “To MD050 on heading 143°M at 2600 ft or above, turn left. To MD051 at 5700 ft or above, turn

⁹<https://ais.enaire.es/AIP/>

left. To RBO at 13000 ft or above, turn right. To PINAR at 13000 ft or above”. Three of the points that define the SID are Area Navigation (RNAV) waypoints whereas one of them is a DVOR/DME Navigational Aid (NAVAID). The geographical coordinates of these points are listed in Table I.

2) Results

The results of the application of the ILC scheme to precise aircraft trajectory tracking in CCO show that precise trajectory tracking is achieved in only three iterations.

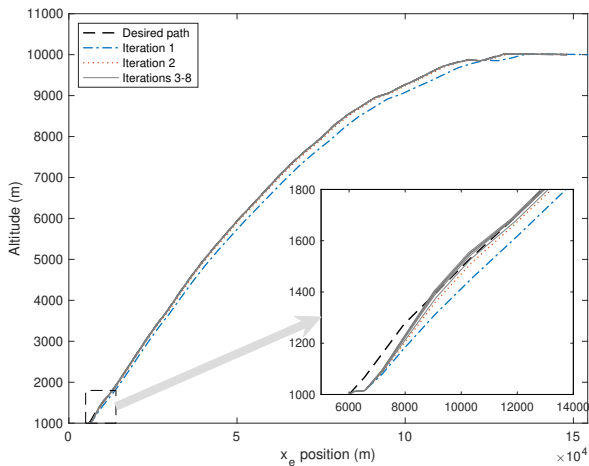
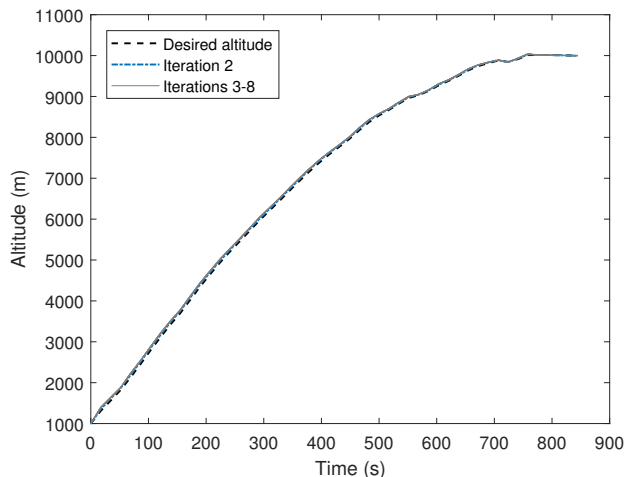


Fig. 4: Evolution of the CCO path $x_e - h_e$ over iterations.

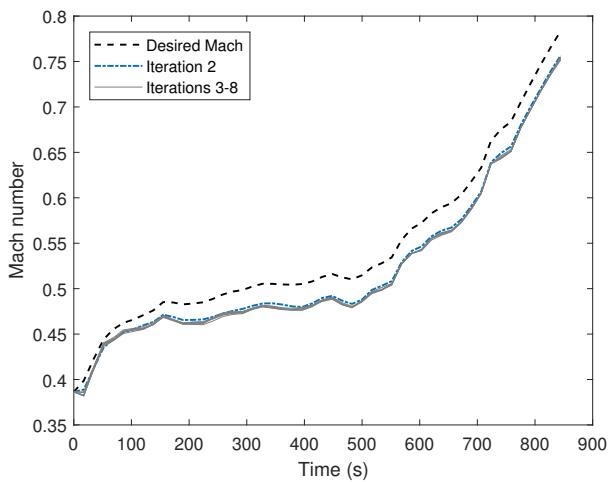
Figure 4 reports the evolution of the tracking of the desired path to perform the CCO obtained in the trajectory planning phase. The desired path is drawn as a dashed black line. In the first iteration, the reference trajectory fed into the flight simulator described above corresponds to the altitude and Mach number obtained in the trajectory planning phase. After each execution, the reference trajectory is updated and the simulated aircraft flies along the paths plotted here.

As shown in Figure 4, the path followed by the aircraft in the first iteration when performing the CCO remains below the desired one until it reaches the cruise level, because of modeling and disturbance errors considered in the flight simulator. Due to the importance of flying through the waypoints with precision, the initial part of the path is shown magnified in the box on the right-hand side of the figure, where it can be observed that the aircraft tracks the desired path with precision from the second iteration. The deviation corresponding to the first portion of the path is due to the dynamics of the feedback controller.

It has already been mentioned that the control paradigm proposed here is nonintrusive with respect to the underlying aircraft feedback controller since it calculates, at each iteration, a reference trajectory for the following aircraft rather than a control input to track the desired trajectory precisely. As explained in Section II-C, the reference trajectory is commanded to the feedback controller of the flight simulator by feeding it with the reference altitude and Mach number, which are depicted in Figure 5 showing that the speed is adjusted in pursuit of precision in the aircraft’s position, while the commanded altitude barely varies along the iterations.



(a) Reference CCO altitude over iterations.



(b) Reference CCO Mach number over iterations.

Fig. 5: Evolution of the CCO reference trajectory over iterations.

As shown in Figure 6, the Mach number in the CCO, depicted in the previous figure, is reduced mainly by increasing the lift coefficient input. It can be seen that the control inputs tend to converge in few iterations. Despite this convergence, both the trajectory and the input vary slightly over iterations due to nonrepetitive disturbances.

The output weighted error in Figure 7 allows the learning performance to be evaluated over iterations. It is calculated as:

$$e_{w,j} = \|S_y y_j\|_2, \quad (16)$$

where S_y is the weighted scaling matrix of the output variables and y_j is the measured output error lifted vector. The output error standard deviation characterizes the system noise level, scaled by S_y . It is obtained from the variations in the trajectory when applying the same input to the aircraft several times.

Although the planned trajectory is feasible in calm wind conditions, it is not when adding wind perturbations. Precision in position has been prioritized over precision in the other state

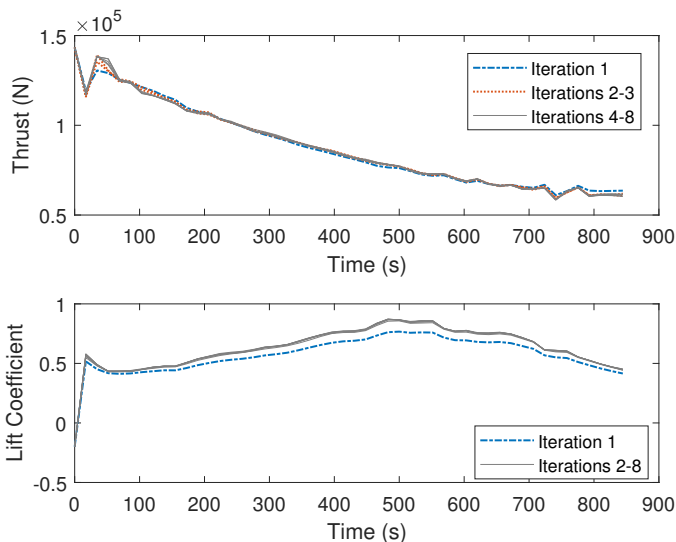


Fig. 6: Evolution of the CCO thrust and lift coefficient over iterations.

variables, and the initial part of the trajectory has been given more importance, penalizing other segments. Therefore, the weighted output error is significantly reduced but does not converge to zero, although it remains near the output error standard deviation, which can be viewed as a lower bound for the achievable tracking error.

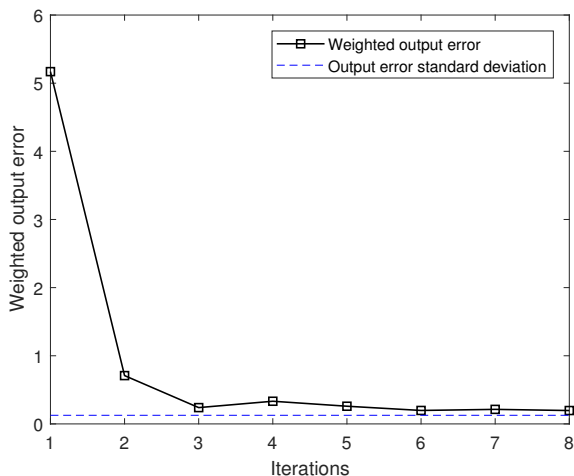


Fig. 7: Evolution of the CCO weighted output error over iterations.

B. Experiment 2: Precise trajectory tracking in a Continuous Descent Operation

In this experiment, the trajectory to be followed by the simulated aircraft is a CDO.

1) Planning the CDO trajectory to be tracked

The general term CDO refers to the operations in which aircraft descend from the cruise altitude to the final approach fix at or near idle thrust, ideally in a low drag configuration, without level segments at low altitude, minimizing the need for

high thrust levels to maintain a constant altitude and reducing the environmental impact of the flight. According to [21], the terms CDO and CDA are interchangeable and should be read and understood in the same context. An optimum CDO starts from the Top-Of-Descent (TOD) and uses descent profiles that reduce controller-pilot communications and segments of level flight. Furthermore, it produces a reduction in noise, fuel burn, and emissions, while increasing flight stability and the predictability of the flight path for both controllers and pilots [23, Chap. 1]. One of the most important requirements for successful CDO operations is predictability, thus precise trajectory tracking is essential.

A generic CDO has been generated in the vertical plane using pseudospectral optimal control techniques to find the trajectory and corresponding control inputs for which the horizontal distance is minimized. It starts at the TOD and continuously descends until reaching an altitude of 2500 m at a speed of 130 m/s. The final conditions of both altitude and speed of the designed trajectory are compliant with a STAR to complete the landing. To ensure that the aircraft reaches these final conditions with precision, the ILC algorithm is tuned to give greater importance to the final part of the trajectory than the rest of it.

2) Results

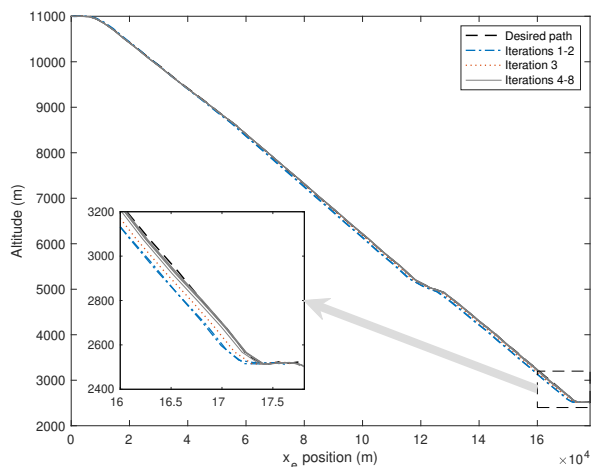
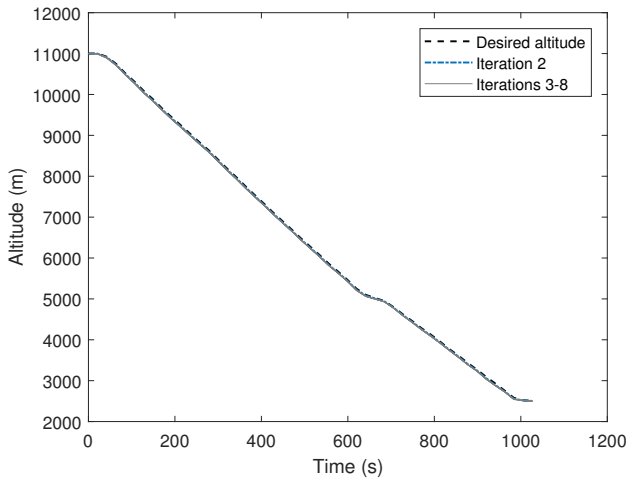


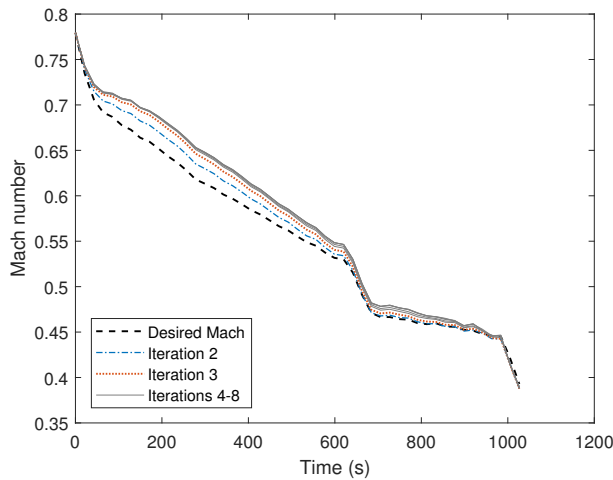
Fig. 8: Evolution of the CDO path $x_e - h_e$ over iterations.

Applying the desired CDO trajectory as the reference trajectory and feeding the flight simulator with the corresponding altitude and Mach number results into the deviations shown in blue in Figure 8, where the dashed black line represents the desired trajectory. In this case, it is important that the final part of the path be followed precisely to undertake the approach phase of the flight. This part is shown magnified in the box on the left-hand side of the figure. Again, the IILC scheme rapidly learns from the first executions, compensating for the recurring disturbances and achieving very precise tracking of the final segment of the CDO trajectory after only two iterations.

As in Experiment 1, the IILC computes a new reference trajectory at each iteration and the reference altitude and Mach number are fed into the feedback controller of the flight simulator. These reference variables are depicted in Figure 9 for the CDO case and, as in the CCO experiment,



(a) Reference CDO altitude over iterations.



(b) Reference CDO Mach number over iterations.

Fig. 9: Evolution of the CDO reference trajectory over iterations.

the speed is adjusted to achieve the required precision in the aircraft's position, while the commanded altitude remains almost unaltered along the iterations.

As shown in Figure 10, the main control action is carried out by the thrust control input, which increases although remaining near idle, while the lift coefficient is reduced. The initial bump in the thrust is due to the dynamics of the feedback controller.

Figure 11 shows the evolution of the weighted output error along the iterations. As in Experiment 1, the weighted output error does not converge to zero since the planned trajectory becomes unfeasible when wind perturbations are integrated into the simulation. Furthermore, the limitations in the thrust control to remain near idle make it more difficult to guide the aircraft along the desired trajectory. Other state variables have been penalized in pursuit of precision in the position of the aircraft, especially in the final segments of the trajectory, where aircraft velocity has been also prioritized. Despite the aforementioned limitations, the weighted output error is reduced by 70% in only three iterations.

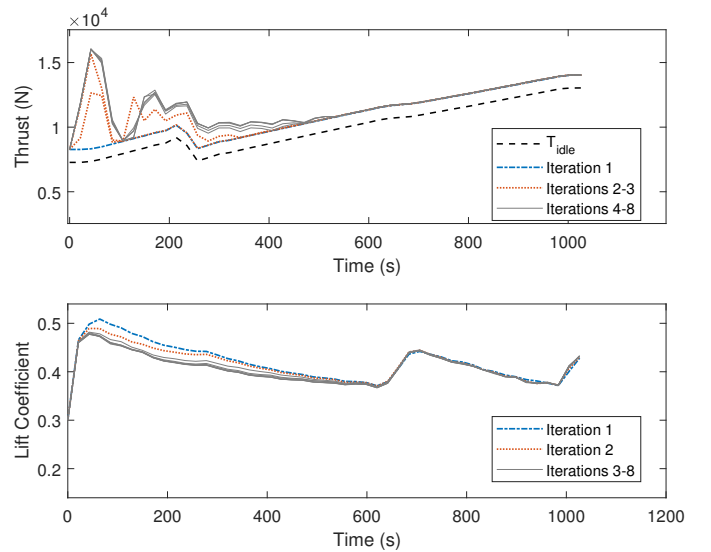


Fig. 10: Evolution of the CDO thrust and lift coefficient over iterations.

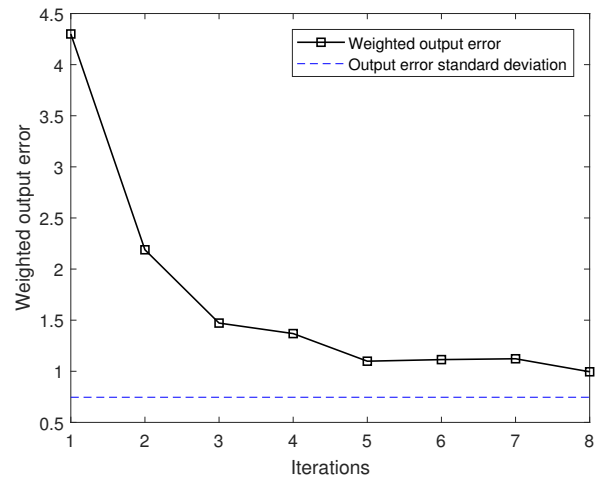


Fig. 11: Evolution of the CDO weighted state error over iterations.

V. CONCLUSION

In this paper, an optimization-based indirect iterative learning control scheme has been applied to aircraft trajectory tracking in continuous climb and descent operations. While the aircraft feedback controller compensates for nonrepetitive disturbances, this method has proven to be very effective in compensating for recurrent disturbances caused mainly by weather and model errors, achieving precise trajectory tracking in few iterations. The simulated environment in which the experiments have been carried out includes a simulator of an Airbus A320 aircraft flying in the vertical plane and a proportional-integral feedback controller which takes the reference Mach number and altitude as inputs to steer the aircraft along a desired trajectory.

This method is especially suitable for aircraft 4D trajectory tracking in departure and arrival procedures at busy airports because, due to the short time separation between flights,

weather conditions and therefore disturbances can be assumed to be similar between consecutive flights, and constraints, which include waypoints and other limitations due to the procedures, can be straightforwardly taken into account.

Moreover, in this method, optimality is pursued in both the estimation of the disturbances and the updating of the reference trajectory and the learning behavior can be adapted depending on the flight phase and precision requirements by assigning different weights to the variables and segments of the trajectory.

The extension of the iterative learning control scheme to the case in which different types of aircraft follow different trajectories in each iteration as well as the improvement of the disturbance estimation method will be the subject of future research.

ACKNOWLEDGMENT

This work has been partially supported by the grants number TRA2017-91203-EXP and RTI2018-098471-B-C33 of the Spanish Government.

REFERENCES

- [1] A. Tewari, *Advanced Control of Aircraft, Spacecraft and Rockets*. Wiley, 2011.
- [2] S. Arimoto, S. Kawamura, and F. Miyazaki, "Bettering operation of robots by learning," *Journal of Robotic Systems*, vol. 1, no. 2, pp. 123–140, 1984.
- [3] K. L. Moore, M. Dahleh, and S. P. Bhattacharyya, "Iterative learning control: A survey and new results," *Journal of Robotic Systems*, vol. 9, no. 5, pp. 563–594, 1992.
- [4] D. A. Bristow, M. Tharayil, and A. Alleyne, "A survey of iterative learning control," *IEEE Control Systems Magazine*, vol. 26, pp. 2039–2114, 2006.
- [5] J.-X. Xu and Y. Tan, *Linear and Nonlinear Iterative Learning Control*. Springer, 2003.
- [6] J.-X. Xu, S. K. Panda, and T. H. Lee, *Real-time Iterative Learning Control: Design and Applications*. Springer, 2009.
- [7] A. P. Schoellig, F. L. Mueller, and R. D'Andrea, "Optimization-based iterative learning for precise quadcopter trajectory tracking," *Autonomous Robots*, vol. 33, no. 1-2, pp. 103–127, 2012.
- [8] O. Purwin and R. D'Andrea, "Performing and extending aggressive maneuvers using iterative learning control," *Robotics and Autonomous Systems*, vol. 59, no. 1, pp. 1–11, 2011.
- [9] X. Liang, M. Zheng, and F. Zhang, "A scalable model-based learning algorithm with application to UAVs," *IEEE Control Systems Letters*, vol. 2, no. 4, pp. 839 – 844, 2018.
- [10] K. L. Moore, M. Johnson, and M. J. Grimble, *Iterative Learning Control for Deterministic Systems*. Springer-Verlag, 1993.
- [11] E. Lavretsky and K. Wise, *Robust and Adaptive Control with Aerospace Applications*. Springer-Verlag, 2013.
- [12] N. Prabhakar, A. Painter, R. Prazenica, and M. Balas, "Trajectory-driven adaptive control of autonomous unmanned aerial vehicles with disturbance accommodation," *Journal of Guidance, Control, and Dynamics*, vol. 41, no. 9, pp. 1976–1989, 2018.
- [13] H. Jafarnejadsani, D. Sun, H. Lee, and N. Hovakimyan, "Optimized l1 adaptive controller for trajectory tracking of an indoor quadrotor," *Journal of Guidance, Control, and Dynamics*, vol. 40, no. 6, pp. 1415–1427, 2017.
- [14] H. Bouadi and F. Mora-Camino, "Modeling and adaptive flight control for quadrotor trajectory tracking," *Journal of Aircraft*, vol. 55, no. 2, pp. 666–681, 2018.
- [15] K. Pereida, R. R. P. R. Duivenvoorden, and A. P. Schoellig, "High-precision trajectory tracking in changing environments through l1 adaptive feedback and iterative learning," in *Proceedings of the 2017 IEEE International Conference on Robotics and Automation*, Marina Bay Sands, Singapore, May-June 2017, pp. 344–350.
- [16] International Civil Aviation Organization, "Global Air Navigation Plan," ICAO, Tech. Rep. 9750-AN/963, 2016.
- [17] A. Buelta, A. Olivares, and E. Staffetti, "Iterative learning control for precise aircraft trajectory tracking in continuous climb operations," in *Proceedings of the Thirteenth USA/Europe Air Traffic Management Research and Development Seminar*, Vienna, Austria, June 2019.
- [18] —, "Iterative learning control for precise aircraft trajectory tracking in continuous descent approaches," in *Proceedings of the 8th European Conference for Aeronautics and Aerospace Sciences*, Madrid, Spain, July 2019.
- [19] Y. Wang, F. Gao, and F. J. Doyle, "Survey on iterative learning control, repetitive control, and run-to-run control," *Journal of Process Control*, vol. 19, no. 10, pp. 1589–1600, 2009.
- [20] V. Mouillet, "User Manual for the Base of Aircraft Data (BADA) Revision 3.14," EUROCONTROL Experimental Centre, Brétigny, France, Tech. Rep., 2017.
- [21] European Organization for the Safety of Air Navigation, "Continuous Descent. A Guide to Implementing Continuous Descent," EUROCONTROL, Tech. Rep., 2011.
- [22] International Civil Aviation Organization, "Continuous Climb Operations (CCO) Manual," ICAO, Tech. Rep. Doc. 9993 AN/495, 2012.
- [23] —, "Continuous Descent Operations (CDO) Manual," ICAO, Tech. Rep. Doc 9931 AN/476, 2010.
- [24] Q. Gong, F. Fahroo, and I. M. Ross, "Spectral algorithm for pseudospectral methods in optimal control," *Journal of Guidance, Control, and Dynamics*, vol. 31, no. 3, pp. 460–471, 2008.
- [25] D. G. Hull, *Fundamentals of Airplane Flight Mechanics*. Springer-Verlag, 2007.
- [26] B. Huang, B. Lu, and Q. Li, "A proportional–integral-based robust state-feedback control method for linear parameter-varying systems and its application to aircraft," *Proceedings of the Institution of Mechanical Engineers, Part G: Journal of Aerospace Engineering*, vol. 233, no. 12, pp. 4663–4675, 2019.
- [27] M. Hadi and N. Abdul, "Reducing the Effect of the Atmospheric Disturbance on Longitudinal Flight Control System Usage PID Controller," *International Journal of Computer Applications*, vol. 127, no. 13, pp. 27–31, 2015.
- [28] M. Peters and M. A. Konyak, "The Engineering Analysis and Design of the Aircraft Dynamics Model For the FAA Target Generation Facility," Federal Aviation Administration, Tech. Rep. 99162-01, 2012.
- [29] D. P. Drob, J. T. Emmert, J. W. Meriwether, J. J. Makela, E. Doornbos, M. Conde, G. Hernandez, J. Noto, K. A. Zawdie, S. E. McDonald, J. D. Huba, and J. H. Klenzing, "An update to the Horizontal Wind Model (HWM): The quiet time thermosphere," *Earth and Space Science*, vol. 2, no. 7, pp. 301–319, 2015.
- [30] U.S. Department of Defense, "The Flying Qualities of Piloted Airplanes," U.S. Federal Government, Tech. Rep. U.S. Military Specification MIL-F-8785C, 1980.
- [31] B. Bamieh, J. B. Pearson, B. A. Francis, and A. Tannenbaum, "A lifting technique for linear periodic systems with applications to sampled-data control," *Systems & Control Letters*, vol. 17, no. 2, pp. 79 – 88, 1991.
- [32] Y. Bar-Shalom, X.-R. Li, and T. Kirubarajan, *Estimation with Applications to Tracking and Navigation*. John Wiley & Sons, 2001.
- [33] D. Simon, "Kalman filtering with state constraints: A survey of linear and nonlinear algorithms," *IET Control Theory Applications*, vol. 4, no. 8, pp. 1303–1318, 2010.
- [34] L. Moin, A. Baig, and V. Uddin, "State space model of an aircraft using Simulink," *International Journal of System Modeling and Simulation*, vol. 2, no. 4, pp. 1–6, 2017.



Almudena Buelta is a Teaching Assistant of Statistics and a PhD student at the Universidad Rey Juan Carlos in Madrid, Spain. She received her MSc degree in Aeronautical Engineering from the Universidad Politécnica de Madrid. She previously worked for Airbus Defence and Space, developing training and operational documentation and providing operational support for in-service aircraft. Her research focuses on iterative learning control applied to commercial aircraft trajectory tracking.



Alberto Olivares is a Professor of Statistics and Vector Calculus at the Universidad Rey Juan Carlos in Madrid, Spain. He received his MSc degree in Mathematics and his BSc degree in Statistics from the Universidad de Salamanca, Spain, and his PhD degree in Mathematical Engineering from the Universidad Rey Juan Carlos. He has worked with the Athens University of Economics and Business. His research interests include statistical learning, stochastic hybrid optimal control and model predictive control with applications to biomedicine, robotics, aeronautics, and astronautics.



Ernesto Staffetti is a Professor of Statistics and Control Systems at the Universidad Rey Juan Carlos in Madrid, Spain. He received his MSc degree in Automation Engineering from the Università degli Studi di Roma “La Sapienza,” and his PhD degree in Advanced Automation Engineering from the Universitat Politècnica de Catalunya. He has worked with the Universitat Politècnica de Catalunya, the Katholieke Universiteit Leuven, the Spanish Consejo Superior de Investigaciones Científicas, and the University of North Carolina at Charlotte. His research interests include stochastic hybrid optimal control, iterative learning control, and model predictive control with applications to robotics, aeronautics, and astronautics.